

# New kind of dodecagonal quasicrystal

Alfredo Metere<sup>1c</sup>, Peter Oleynikov<sup>1</sup>, Mikhail Dzugutov<sup>2</sup> and Sven Lidin<sup>3</sup>

<sup>1</sup> *Department of Materials and Environmental Chemistry,*

*Stockholm University, Arrhenius Väg. 16C S-10691 Stockholm, Sweden*

<sup>2</sup> *Department of Mathematics, Royal Institute of Technology, SE-100 44 Stockholm, Sweden*

<sup>3</sup> *Division of Polymer & Materials Chemistry Lund University SE-221 00 Lund Sweden*

(Dated: April 16, 2015)

We report a novel kind of dodecagonal quasicrystal that has so far never been observed, nor theoretically predicted. It is composed of axially stacked hexagonal particle layers, with 12-fold rotational symmetry induced by  $30^\circ$  rotation of adjacent layers with respect to each other. The quasicrystal was produced in a molecular-dynamics simulation of a single-component system of particles interacting via a spherically-symmetric potential, as a result of a first-order phase transition from a liquid phase under constant-density cooling. This finding implies that a similarly structured quasicrystal can possibly be produced by the mesogens of the kind that produce smectic-B crystals and in a system of spherically-shaped colloidal particles with appropriately tuned potential.

PACS numbers: 61.44.Br, 61.44.-n, 83.10.Rs

Quasiperiodic order in mesoscopic soft-matter systems is now a new research frontier of rapidly growing interest [1]. First of all, the interest in the studies of mesoscopic-scale soft-matter quasicrystals is motivated by the perspective application of mesoscopic quasicrystals in photonics [2]. Following the first discovery of a dodecagonal quasicrystal in a micelle-forming system [3], similar structures were produced in colloids [4], mesoporous silica [5], binary system of nanoparticles [6] and star polymers [7]. Soft-matter quasicrystals were also simulated using molecular dynamics [8]. However, the structure of all these quasicrystals reproduces, on mesoscopic scale, the tetrahedrally close-packed structure of the quasicrystals observed in intermetallic compounds. One independent way to induce quasiperiodic order to be mentioned is superposition of Faraday waves [9].

In this context, mesogenic systems forming smectic phases [10] are of particular interest. These phases, usually composed of elongated particles, exhibit layered structures with uniaxial particle orientation [10, 11]. So far, the only kind of quasiperiodic order observed in smectic phases has been twist grain boundaries (TGB) structure, where the layers in adjacent structural blocks are commensurately rotated by an appropriate angle around a helical axis parallel to the layers [12, 13].

Smectic mesophases commonly solidify into the 6-fold smectic-*B* crystal which represents a uniaxial stacking of coherently oriented hexagonally close-packed layers [11, 14]. Here, we report a novel type of solid smectic phase possessing 12-fold symmetry produced in a molecular-dynamics simulation of a simple one-component system. Like the smectic-B crystal, it consists of hexagonally ordered layers axially stacked in *ABA* order, but in contrast to the crystal, its *A* and *B* layers are rotated by  $30^\circ$  with respect to each other, in the layer plain. This is a new smectic solid phase, and a new type of quasicrystal that has never been observed in other systems, nor theoretically predicted.

The molecular-dynamics model we utilized in this study consists of 16384 identical particles confined to a cubic box with periodic boundary conditions. The interparticle interaction was assumed to be spherically-symmetric, described by the pair potential (see Methods).

We investigated the system's phase behaviour under temperature variation at the constant number density  $\rho = 0.32$ . The temperature was changed in a stepwise manner, with comprehensive equilibration of the system at a new temperature after each step. At the beginning, the system was equilibrated in its thermodynamically stable isotropic liquid state at sufficiently high temperature, after which it was subjected to isochoric cooling.

Fig. 1 presents the system's energy and pressure variations as functions of temperature at the number density  $\rho = 0.32$ . A discontinuous change in the thermodynamic parameters was detected as the liquid had been cooled below  $T = 1.1$ . It was also found that this thermodynamic singularity was accompanied by a sharp drop in the rate of self-diffusion. These discontinuities convincingly demonstrate that the system performed under cooling a first-order phase transition from the liquid state to a solid phase. This conclusion can be confirmed by a significant hysteresis that was observed when re-heating the low-temperature phase, see Fig. 1. A non-trivial character of the produced low-temperature solid phase was indicated by an anomalously long time required for its equilibration which amounted to about a billion of time-steps.

The structure characterisation of the low-temperature solid phase has been performed by inspecting the reciprocal-space pattern of its density distribution. For that purpose, we calculated the structure factor  $S(\mathbf{Q})$  (see Methods) which represents the scattered beam intensity as measured in the diffraction experiments. To remove thermally induced fluctuations, the simulated configuration was subjected to the steepest descent energy

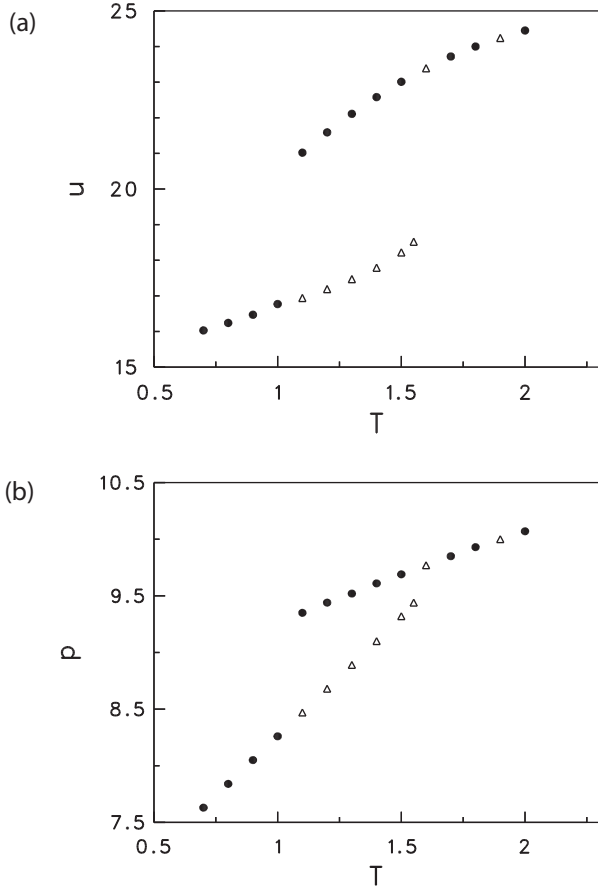


FIG. 1: Liquid-solid phase transformation. (a) and (b), respectively: the temperature variation of the energy and pressure at the number density  $\rho = 0.32$ . Dots: cooling; triangles: heating.

minimisation which mapped it onto the nearest minimum of its energy landscape. This minimum was found to correspond to the number density  $\rho = 0.31$ .

As a first step in this structure analysis, we determine the global symmetry of the configuration, and its axis orientation (see Methods). The latter having been found, we calculated  $S(\mathbf{Q})$  on the reciprocal-space plane  $Q_z = 0$ ,  $Q_z$  being the axis coordinate; this result is presented in Fig. 2a. The pattern of  $S(\mathbf{Q})$  maxima observed in that  $\mathbf{Q}$  plane is distinctively 12-fold. To further demonstrate the 12-fold rotational invariance of the simulated configuration, we also calculated the structure factor in two planes defined by the axis and two translational symmetry vectors,  $30^\circ$  apart, which are indicated in Fig. 2a. The results, shown in Fig. 2b, are indeed consistent with the conclusion that the reciprocal-space image of the simulated structure is invariant with respect to  $30^\circ$  rotation.

Besides, the two diffraction patterns in Fig. 2b look like those observed in typical smectic-B crystals [14, 15]. They represent a structure composed of flat close-packed particle layers axially stacked in *ABA* order [16]. The

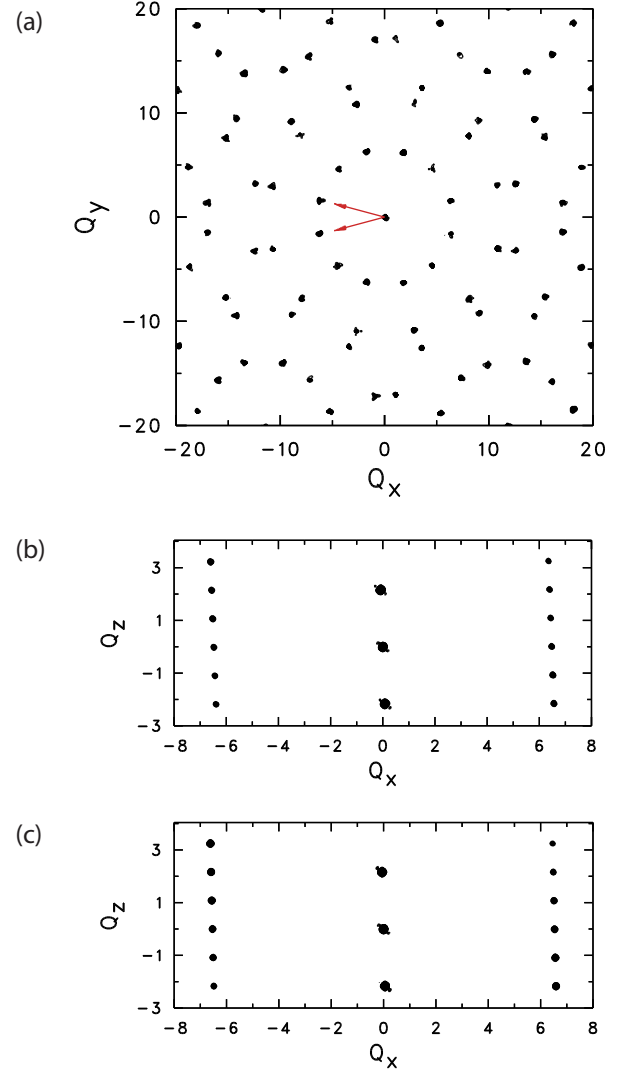
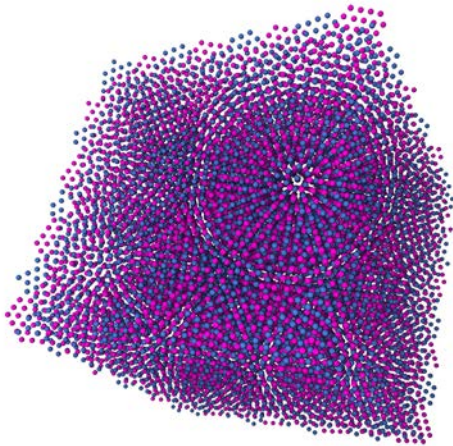


FIG. 2: Isointensity contour plots of the structure factor  $S(\mathbf{Q})$  (see Methods). (a): in the  $\mathbf{Q}$ -plane perpendicular to the axis. (b) and (c) represent respectively two  $\mathbf{Q}$ -planes defined by the axis and the two vectors,  $30^\circ$  apart, shown in the top panel.

diffraction results in Fig. 2b also make it possible to estimate the ratio of the interlayer spacing and the interparticle distance within a layer as about 3, which can be compared with the aspect ratio of constituent particles in commonly occurring smectic phases. We note that this value is consistent with the ratio of the positions of two minima in the pair potential, see Fig. 1a. Thus, the configuration is structurally similar to the smectic-B crystal, except that, in contrast to hexagonal symmetry of the latter, it exhibits 12-fold symmetry.

These diffraction results can be interpreted by assuming that the system's apparent 12-fold axial symmetry is induced by  $30^\circ$  rotation of the *A* and *B* subsystems of layers with respect to each other, in the layer plane. This

(a)



(b)

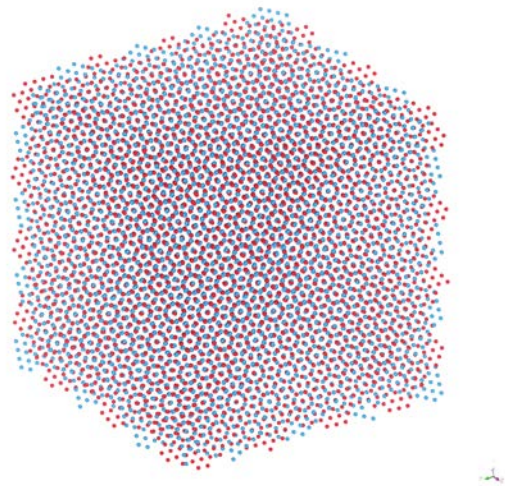


FIG. 3: An axial view of the configuration. (a): perspective projection. (b): orthogonal projection. Adjacent A and B layers are discriminated by color.

conclusion is supported by the visual inspection of the real-space images of the simulated structure presented in Fig. 3. The view from the axial direction, Fig. 3a, shows a pattern of 12-particle rings characteristic of dodecagonal structures [17, 18], and its particle density lines that can be detected by looking at the grazing angle exhibit  $30^\circ$  rotational invariance. When viewed along the layer plane, Fig. 3b, the configuration looks like a typical smectic-B crystal with  $ABA\dots$  layer stacking; its only distinction from the latter is that the adjacent A and B layers are rotated with respect to each other, in the layer plane, by  $30^\circ$ . This can also be seen in Fig. 3c.

In Fig. 4 we present tiling of the axial projection of two adjacent layers of the quasicrystal. The tiling is

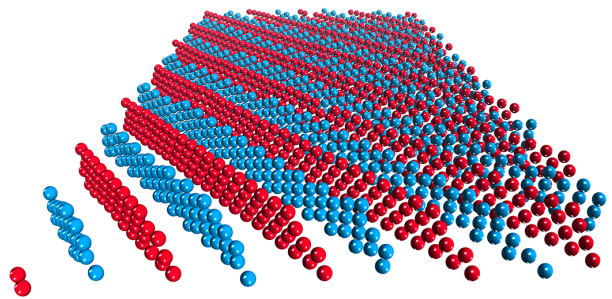


FIG. 4: A slice of the configuration cut parallel to the axis.

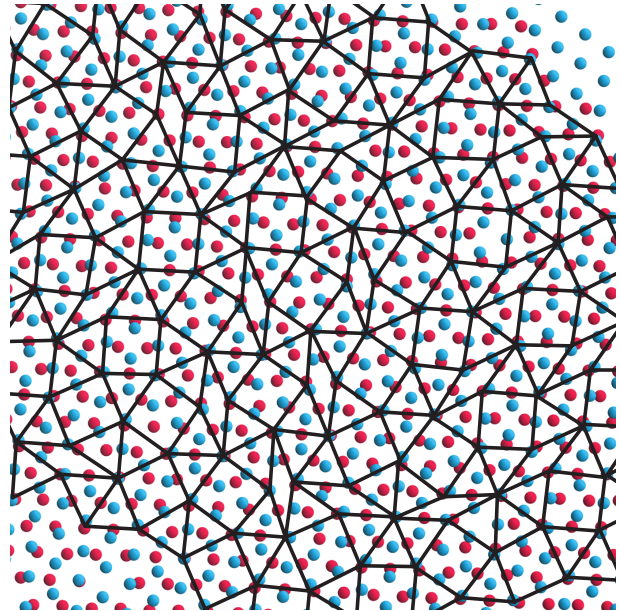


FIG. 5: Tiling of the axial projection of two adjacent particle layers, produced by connecting centres of adjacent 12-particle rings.

produced by connecting the centres of adjacent apparent 12-particle rings which the pattern is composed of. Besides equilateral triangles and squares, typical for periodic tilings, the present tiling includes the  $30^\circ$  rhombus, an element specific for a 12-fold tiling pattern [17, 18].

In crystallographic classification, the symmetry of this quasicrystal is  $P12_6/mmc$ . The quasicrystal is composed of stacked layers of  $6^3$  nets that each have planar  $6mm$  symmetry. The stacking along the axis with a  $\pi/6$  relative rotation of the adjacent layers preserve the mirror operations and subsequent layers are related by a  $12_6$  screw operation and a diagonal glide reflection with a  $1/2c$  component. We note that the screw operation producing this structure results in extinction of some reflections in its diffraction pattern which are characteristic of the diffraction patterns of conventional tetrahedrally close-packed dodecagonal quasicrystals, e.g. those found in intermetallic systems [19]. In this respect, it should be mentioned that the diffraction pattern of the present

structure, Fig. 2a, is identical to that of the twinned multidomain fcc structure produced by staking of 6-fold domains alternate  $0^\circ, 30^\circ$ -rotated in 111 plane [4]. In this way, the present structure is conceptually similar to the quasicrystalline TGB phases which too give rise to the diffraction patterns that differ significantly from those observed in conventional quasicrystals.

Thus, we found a new type of smectic quasicrystalline phase, alternative to the TGB quasicrystals. The new phase differs from the latter in real-space structure while resembling it in terms of general concept. The new quasicrystal can possibly be classified as a *dodecagonal smectic-B* phase.

A conceptually significant peculiarity of the simulated smectic quasicrystal is that it exhibits complete absence of local phason disorder. That the layers are perfectly identical can be concluded by inspecting the general view of the configuration from the axial direction which is presented in Figure 3. This feature appears to be a generic property of this quasicrystal due to its physical nature, and the way of its layer stacking. Due to the strong interaction between particles within a layer induced by the first minimum in the potential, Figure 1, the hexagonal layer structure is solid, making the energy cost for intralayer dynamics forbiddingly high. Thus, this quasicrystal structure represents a single energy minimum, which excludes any possibility for energetically degenerate local phason flips[20]. The absence of phason dynamics, and its respective entropic contribution to the free energy [21] implies that the mechanism of thermodynamic stability of this quasicrystal is entirely energetic, which suggests that this structure might be considered as a candidate for the quasiperiodic ground state.

On the other hand, this configuration, constrained by periodic boundary conditions, is a periodic approximant, and the absence of local phason dynamics implies the presence of a uniform phason strain which can be observed both in the diffraction pattern and by inspecting the density lines in the real-space configuration, Fig. 3a, at a grazing angle. It arises from the fact that each of the two subsets of 6-fold periodic layers must independently be oriented consistently with the periodic boundaries. Therefore, the rotation angle between the two cannot be exactly  $30^\circ$ , and the deviation is size-dependent.

Two possible ways of materialization of this structure in real physical systems can be conjectured. First, the morphological similarity of the simulated smectic quasicrystal and the smectic-B crystal strongly suggests that some mesogens of those forming the latter phase may also be able to freeze into a quasiperiodic structure like the one we report here. Moreover, these mesogens may also form a liquid-crystal “dodecatic” mesophase that was recently suggested [22] as a dodecagonal counterpart of the 6-fold hexatic mesophase. It is suggested to possess 12-fold symmetry both in the local positional order and in its global bond-orientational order.

Second, the main features of the spherically-symmetric interparticle potential used in the present model show similarity to the force field predicted for colloidal systems by the classical Deryagin-Landau-Verwey-Overbeek theory [23, 24] (amended with hard core repulsion or steric repulsion at close to contact). This suggests a possibility that smectic-like layered structures exhibiting dodecagonal symmetry similar to the one reported here can be produced in colloidal systems of spherically shaped particles, with appropriate tuning of the effective potential.

In summary, we report a molecular-dynamics simulation demonstrating that a system of identical particles interacting via a spherically-symmetric potential can form a phase morphologically similar to the smectic-B crystal but possessing 12-fold symmetry. This is a new kind of smectic quasicrystal, alternative to the quasicrystalline TGB phases which it resembles in terms of the general design principle. This finding opens a perspective of producing similar quasicrystals in the mesogens that are known to form the smectic-B crystals. Conceptually, it introduces a new formation mechanism of quasiperiodic order. It also changes the basic model of smectic phases, thereby advancing our understanding of the causes underlying the occurrence of particular structures in the phase transformations of liquid crystals.

## APPENDIX: METHODS

### Pair potential

The pair potential used in this simulation is shown in Fig. 5.

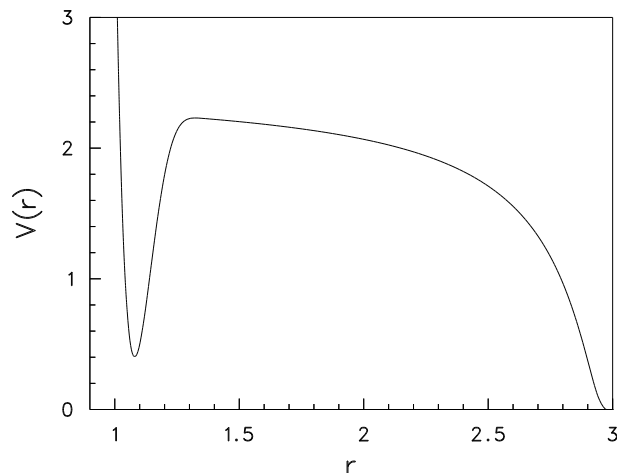


FIG. 6: Pair potential

The functional form of the potential energy for two particles separated by the distance  $r$  is:



$$V(r) = a_1(r^{-m} - d)H(r, b_1, c_1) + a_2H(r, b_2, c_2) \quad (1)$$

where

$$H(r, b, c) = \begin{cases} \exp\left(\frac{b}{r-c}\right) & r < c \\ 0 & r \geq c \end{cases} \quad (2)$$

m	a <sub>1</sub>	b <sub>1</sub>	c <sub>1</sub>	a <sub>2</sub>	b <sub>2</sub>	c <sub>2</sub>	d
12	265.85	1.5	1.45	2.5	0.19	3.0	0.8

TABLE I: Values of the parameters for the pair potential.

The values of the parameters are presented in Table I. The first term describes the short-range repulsion, and the minimum, whereas the second term expresses the long-range repulsion. All the quantities we report here are expressed in terms of the reduced units that were used in the definition of the potential. Note that its short-range repulsion part, and the position of the minimum, are consistent with those of the Lennard-Jones (LJ) potential [25], which makes it possible to compare the reduced number densities of the two systems.

This pair potential represents a modification of an earlier reported pair potential [15] that was found to produce the smectic-B crystal. The main difference between these two potentials is that in present one the long-range repulsion branch is extended to a significantly larger distance. This modification was intended to increase spacing between the layers, thereby reducing the interlayer cohesion.

### Structure characterisation

In the reciprocal space, the structure of a simulated system of particles is presented in terms of static structure factor  $S(\mathbf{Q})$  that is defined as

$$S(\mathbf{Q}) = \langle \rho(\mathbf{Q})\rho(-\mathbf{Q}) \rangle \quad (3)$$

where  $\rho(\mathbf{Q})$  is the  $\mathbf{Q}$ -component of the spatial Fourier-transform of the instantaneous number density distribution of a system of  $N$  particles:

$$\rho(\mathbf{Q}, t) = \frac{1}{\sqrt{N}} \sum_{i=1}^N \exp[-i\mathbf{Q}\mathbf{r}_i] \quad (4)$$

$\mathbf{r}_i$  being the position of particle  $i$ , and  $\langle \rangle$  denoting ensemble averaging.

A spherically-averaged static structure factor can be calculated [25] from the spherically invariant radial distribution function  $g(r)$  as:

$$S(Q) = 1 + 4\pi\rho \int_0^\infty [g(r) - 1] \frac{\sin(Qr)}{Qr} r^2 dr \quad (5)$$

As a first step in this structure analysis, we calculated  $S(\mathbf{Q})$  on the reciprocal-space sphere of the radius corresponding to the position of the first peak of the spherically averaged structure factor (see Methods). That calculation produced a pattern of well-defined  $S(\mathbf{Q})$ -maxima, which represent decomposition of the peak of the spherically averaged structure factor on thus defined  $\mathbf{Q}$ -sphere. This made it possible to determine the global symmetry of the configuration, and the axis orientation.

- 
- [1] J.-M. Dubois, and R. Lifshitz, *R. Phil. Mag.*, **91** 2971 (2011)
  - [2] Z. Valy Vardeny, A. Nahata, and A. Agrawal, *Nature Photonics* **7**, 177 (2013)
  - [3] X. Zeng, G. Ungar, Y. Liu, V. Percec, A.E. Dulcey, and J.K. Hobbs, *J.K.*, *Nature* **428**, 157 (2004)
  - [4] S. Fischer, A. Exnera, K. Zielskea, J. Perlich, S. Deloudic, W. Steurer, and S. Forster, *PNAS*, 10.1073/pnas.1008695108 (2011)
  - [5] C. Xiao, N. Fujita, K. Miyasaka, Y. Sakamoto, and O. Terasaki, *Nature* **487** 349 (2012)
  - [6] D.V. Talapin, E.V. Shevchenko, M.I. Bodnarchuk, X. Ye, J. Chen, and C.B. Murray, *Nature* **461** 964 (2009)
  - [7] K. Hayashida, T. Dotera, A. Takano, and Y. Matsushita, *Phys. Rev. Lett.* **98** 195502 (2007)
  - [8] C.R. Iacovella, A.S. Keys, and S. Glotzer, *PNAS*, **108**, 20935 (2011)
  - [9] R. Lifshitz, and D.M. Petrich, *Phys. Rev. Lett.*, **79**, 1261 (1997)
  - [10] S. Chandrasekhar, *Liquid Crystals, Cambridge University Press, Cambridge* (1992).
  - [11] P. Bolhuis, and D. Frenkel, *J. Chem. Phys* **106** 666 (1997)
  - [12] S.R. Renn, and T.C. Lubensky, *Physical Review A* **38**, 2132 (1988)
  - [13] J.W. Goodby, M.A. Waugh, S.M. Stein, E. Chin, R. Pindak, J.S. Patel, *Nature*, **337**, 449 (1989)
  - [14] A. J. Leadbetter, M.A. Mazid, B.A. Kelly, J.W. Goodby, and G.W. Gray, *Phys. Rev. Lett.* **43**, 630 (1979)
  - [15] A. Metere, T. Oppelstrup, S. Sarman, A. Laaksonen, M. Dzugutov, *Phys. Rev. E* **88**, 062502 (2013)
  - [16] A.J. Leadbetter, J.C. Frost, et M.A. Mazid, *J. Physique Lett.* **40**, (1979)
  - [17] F. Gähler, *Crystallography of Dodecagonal Quasicrystals in Quasicrystalline Materials, Ch. Janot and J.M. Dubois (eds.), World Scientific* (1988).
  - [18] M. Dzugutov, *Phys. Rev. Lett.* **70**, 2924-2928 (1993)
  - [19] T. Ishimasa, *Isr. J. Chem.* **51**, 1216 (2011)
  - [20] M. Dzugutov, *Europhys. Lett.*, **31**, 95 (1995)
  - [21] M.E.J. Newman, and C.L. Henley, *Phys. Rev. B* **52**, 6386 (1995).
  - [22] T. Dotera, *Journ. of Polymer Science B: Polymer Physics* **50**, 155 (2011)
  - [23] E.J. Verwey, and J.T.H.G. Overbeek, *Theory of the stability of lyophobic colloids, Amsterdam, Elsevier* (1948)
  - [24] J.N. Israelachvili, *Intermolecular and Surface Forces*, 3rd edition, *Academic Press* (2011)
  - [25] J.-P. Hansen, and I.R. McDonald, *Theory of simple liquids, Academic Press* (2006)